Spectroelectrochemical Studies on Mixed-Valence States in a Cyanide-Bridged Molecular Square, $[Ru^{II}_2Fe^{II}_2(\mu\text{-}CN)_4(bpy)_8](PF_6)_4 \cdot CHCl_3 \cdot H_2O$

Hiroki Oshio,*[a] Hironori Onodera,[b] and Tasuku Ito[b]

Abstract: A cyanide-bridged molecular square of $[Ru^{II}_2Fe^{II}_2(\mu\text{-}CN)_4(bpy)_8](PF_6)_4 \cdot CHCl_3 \cdot H_2O$, abbreviated as $[Ru^{II}_2Fe^{II}_2](PF_6)_4$, has been synthesised and electrochemically generated mixed-valence states have been studied by spectroelectrochemical methods. The complex cation of $[Ru^{II}_2Fe^{II}_2]^{4+}$ is nearly a square and is composed of alternate Ru^{II} and Fe^{II} ions bridged by four cyanide ions. The cyclic voltammogram (CV) of $[Ru^{II}_2Fe^{II}_2](PF_6)_4$ in acetonitrile showed four quasireversible waves at 0.69, 0.94, 1.42 and 1.70 V (vs. SSCE), which correspond to the four one-electron redox processes of $[Ru^{II}_2Fe^{II}_2]^{4+} \rightleftarrows [Ru^{II}_2Fe^{II}Fe^{III}]^{5+} \rightleftarrows [Ru^{II}_2Fe^{III}_2]^{6+} \rightleftarrows [Ru^{II}Ru^{III}Fe^{III}_2]^{7+} \rightleftarrows [Ru^{III}_2Fe^{III}_2]^{8+}$. Electrochemically generated $[Ru^{II}_2Fe^{II}Fe^{III}]^{5+}$ and $[Ru^{II}_2Fe^{III}_2]^{6+}$ showed new absorption bands at 2350 nm ($\varepsilon = 5500\,M^{-1}\,cm^{-1}$) and 1560 nm ($\varepsilon = 10500\,M^{-1}\,cm^{-1}$), respectively, which were assigned to the intramolecular IT (intervalence transfer) bands from Fe^{II} to Fe^{III} and from Ru^{II} to Fe^{III} ions, respectively. The electronic interaction matrix elements (H_{AB}) and the degrees of electronic delocalisation (α^2) were estimated to be 1090 cm^{-1} and 0.065 for the $[Ru^{II}_2Fe^{II}Fe^{III}_2]^{5+}$ state and 1990 cm^{-1} and 0.065 for the $[Ru^{II}_2Fe^{III}_2]^{6+}$ states.

Keywords: cyanometalate · electrochemistry · iron · mixed-valent compounds · molecular square · ruthenium

Introduction

Cyanide-bridged transition-metal compounds show various physical properties such as electrochromism, photo- and chemically induced phase transitions and magnetism,[1] which are characteristic properties of solids and discrete molecules. A series of cyanide-bridged infinite systems formulated as $M_x[M'(CN)_y]$ (M and M′ are transition metal ions, $y = 6$ or 7) have been shown to be bulk magnets,[2] and some showed photoinduced magnetic-ordering phenomena.[3] Cyanometalates of $[M(CN)_6]^{n+}$ and $[M(CN)_8]^{n+}$ have been used to construct molecular architectures with high-spin ground states[4] such as heptanuclear $[Cr^{III}Mn^{II}_6]$ ($S = 27/2$) and $[Cr^{III}Ni^{II}_6]$ ($S = 15/2$),[5] and higher nuclearites $[Mn^{II}_9W^{V}_6]$ ($S = 39/2$) and $[Mn^{II}_6Mo^{V}_9]$ ($S = 51/2$).[6] Because it is possible to exert some synthetic control by using cyanide complexes, larger cluster complexes $[Cr^{III}_{12}Ni^{II}_{12}(CN)_{48}]^{12+}$ and $[Cr^{III}_{14}Ni^{II}_{13}(CN)_{48}]^{20+}$ have been prepared and are expected to have superparamagnetic behaviour.[7] Metal complexes that have metal ions in different valence states can give rise to strong electronic interactions such as intervalence charge transfer (IVCT). For valence-localised systems, the energy of the IVCT band is equal to the sum of the reorganisation energy and the ground-state free-energy difference, and the magnitude of the electronic coupling (H_{AB}) is inferred from the oscillator strength of the IVCT band obtained by spectroelectrochemical methods. Despite the diverse potential applications of cyanometalates, relatively little is known about the properties of IVCT interactions in mixed-metal systems. The development of versatile synthetic routes to prepare mixed-metal clusters provides an opportunity to study the interactions in these systems. We have been studying a class of cyanide-bridged cluster molecules with a general formula of $[Fe_2M_2(\mu\text{-}CN)_4(bpy)_6]^{n+}$ (bpy = 2,2′-bipyridine) in which cyanide ions bridge four metal ions to form the macrocyclic tetranuclear core, so-called molecular squares. In this paper we present the synthesis, crystal structure and spectroelectrochemical studies of $[Ru^{II}_2Fe^{II}_2(\mu\text{-}CN)_4(bpy)_8](PF_6)_4 \cdot CHCl_3 \cdot H_2O$.

[a] Prof. H. Oshio
Department of Chemistry, University of Tsukuba
Tennodai 1-1-1, Tsukuba 305-8751 (Japan)
Fax: (+81) 298-53-4238
E-mail: oshio@chem.tsukuba.ac.jp

[b] H. Onodera, Prof. T. Ito
Department of Chemistry, Graduate School of Science
Tohoku University, Aoba-ku, Sendai 980-8578 (Japan)
Fax: (+81) 22-217-6544
E-mail: ito@agnus.chem.tohoku.ac.jp

Results and Discussions

Synthesis and description of the structure: The reaction of $[Fe(CN)_2(bpy)_2]$ with $[Ru(bpy)_2(solvent)_2]^{2+}$ yielded a tetra-

DOI: 10.1002/chem.200304867

nuclear complex of $[Ru^{II}_2Fe^{II}_2(\mu\text{-}CN)_4(bpy)_8](PF_6)_4 \cdot CHCl_3 \cdot H_2O$, abbreviated as $[Ru^{II}_2Fe^{II}_2](PF_6)_4$. The molecular structure of $[Ru^{II}_2Fe^{II}_2]^{4+}$ is shown in Figure 1, and selected bond lengths and angles are listed in Table 1.

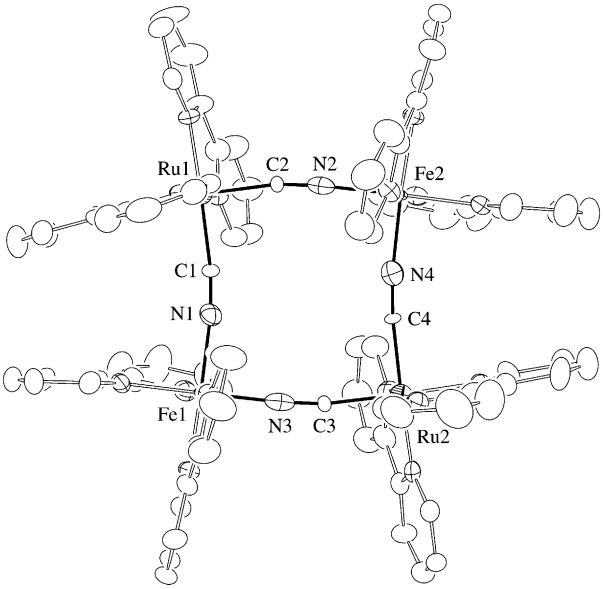

Figure 1. Ortep diagram (30% probability) of the square cation in $[Ru^{II}_2Fe^{II}_4(\mu\text{-}CN)_4(bpy)_8](PF_6)_4 \cdot CHCl_3 \cdot H_2O$. Hydrogen atoms are omitted for clarity.

Table 1. Selected bond lengths [Å] and angles [°] for $[Ru_2Fe_2(\mu\text{-}CN)_4(bpy)_8](PF_6)_4 \cdot CHCl_3 \cdot H_2O$

Ru(1) – C(2)	1.970(9)	Ru(1) – C(1)	1.985(9)
Ru(1) – N(8)	2.007(8)	Ru(1) – N(6)	2.009(8)
Ru(1) – N(7)	2.017(9)	Ru(1) – N(5)	2.042(7)
Ru(2) – C(4)	1.955(9)	Ru(2) – C(3)	1.971(9)
Ru(2) – N(12)	2.015(8)	Ru(2) – N(10)	2.021(9)
Ru(2) – N(9)	2.035(9)	Ru(2) – N(11)	2.042(8)
Fe(1) – N(1)	1.965(9)	Fe(1) – N(3)	1.980(11)
Fe(1) – N(14)	1.996(8)	Fe(1) – N(13)	1.997(8)
Fe(1) – N(16)	2.009(9)	Fe(1) – N(15)	2.022(8)
Fe(2) – N(4)	1.966(9)	Fe(2) – N(20)	1.987(9)
Fe(2) – N(2)	1.999(10)	Fe(2) – N(18)	2.006(9)
Fe(2) – N(17)	2.012(9)	Fe(2) – N(19)	2.013(7)
N(1) – C(1)	1.130(11)	N(2) – C(2)	1.141(12)
N(3) – C(3)	1.153(12)	N(4) – C(4)	1.168(11)
Ru(1)···Fe(1)	5.0484(15)	Ru(1)···Fe(2)	5.0810(16)
Ru(2)···Fe(2)	5.0629(15)	Ru(2)···Fe(1)	5.0746(16)
C(2)-Ru(1)-C(1)	88.7(4)	C(4)-Ru(2)-C(3)	89.8(4)
N(1)-Fe(1)-N(3)	89.0(3)	N(4)-Fe(2)-N(2)	89.8(4)
C(1)-N(1)-Fe(1)	172.6(8)	C(2)-N(2)-Fe(2)	175.1(8)
C(3)-N(3)-Fe(1)	174.9(8)	C(4)-N(4)-Fe(2)	171.6(9)
N(1)-C(1)-Ru(1)	172.1(9)	N(2)-C(2)-Ru(1)	170.9(8)
N(3)-C(3)-Ru(2)	170.4(8)	N(4)-C(4)-Ru(2)	174.9(8)

$[Ru^{II}_2Fe^{II}_2](PF_6)_4$ crystallised in triclinic space group $P\bar{1}$, and the complex cation resides on a centre of symmetry. $[Ru^{II}_2Fe^{II}_2]^{4+}$ is a nearly square tetranuclear macrocycle with alternating Ru^{II} and Fe^{II} ions at the corners of the square. Magnetic susceptibility measurements revealed that both metal ions are diamagnetic. The opposite pairs of cyanide are arranged in an anti-parallel fashion to each in order to bridge neighbouring metal ions and have flipped during the course of the reaction. The positions of the Ru^{II} ions were assigned to the highest peaks found in the direct method (SHELEX-97), but the assignments of the metal ions and the orientation of the cyanide moieties are ambiguous from the X-ray analysis alone. However, comparison of the CV data for $[Ru^{II}_2Fe^{II}_2]^{4+}$ and a related ferrous square, $[Fe^{II}_4(\mu\text{-}CN)_4(bpy)_8](PF_6)_4$,[8] (abbreviated as $[Fe^{II}_4](PF_6)_4$) supports the assignments; this will be discussed later. The Ru^{II} and Fe^{II} ions in the square have a quasioctahedral coordination geometry, of which four coordination sites are occupied by two bpy ligands and the remaining two *cis* positions are coordinated by cyanide ions. It is interesting to compare the core structures of $[Ru^{II}_2Fe^{II}_2](PF_6)_4$ with $[Fe^{II}_4](PF_6)_4$.[8] In $[Ru^{II}_2Fe^{II}_2](PF_6)_4$ the coordination bond lengths of Ru^{II}–C(cyanide) and Fe^{II}–N(cyanide) are 1.955(9) – 1.985(9) Å and 1.965(9) – 1.987(9) Å, respectively, while in $[Fe^{II}_4](PF_6)_4$ the Fe^{II}–C(cyanide) and Fe^{II}–N(cyanide) distances are in the range 1.899(4) – 1.927(4) Å and 1.929(4) – 1.950(4) Å, respectively. The triple-bond lengths of the cyanide groups for $[Ru^{II}_2Fe^{II}_2](PF_6)_4$ are 1.130(11) – 1.168(11) Å, and the corresponding lengths found in $[Fe^{II}_4](PF_6)_4$ are 1.144(6) – 1.154(4) Å. The M–N(bpy) bond lengths are longer in $[Ru^{II}Fe^{II}](PF_6)_4$ (2.015(8) – 2.042(8) Å) than in $[Fe^{II}_4](PF_6)_4$ (1.950(4) – 1.981(4) Å) due to greater π-back donation in the $[Fe^{II}_4](PF_6)_4$ square. The C-Ru^{II}-C and N-Fe^{II}-N bond angles are close to 90° (88.7(4) – 89.8(4)°), and the Ru^{II}-C-N and Fe^{II}-N-C bond angles are 170.4(8) – 174.9(8)°. In $[Ru^{II}_2Fe^{II}_2](PF_6)_4$ the cyanide bridges separate the Ru^{II} and Fe^{II} ions with interatomic distances of 5.048(2) – 5.081(2) Å, while the corresponding distances in $[Fe^{II}_4](PF_6)_4$ are 4.947(1) – 4.986(1) Å. Individual squares are chiral, with the metal ions having either *ΛΛΛΛ* or *ΔΔΔΔ* configurations.

Electrochemistry: A cyclic voltammogram (CV) of $[Ru^{II}_2Fe^{II}_2](PF_6)_4$, measured in acetonitrile, is shown in Figure 2. Table 2 summarises the CV data for $[Ru^{II}_2Fe^{II}_2](PF_6)_4$ together with related compounds.

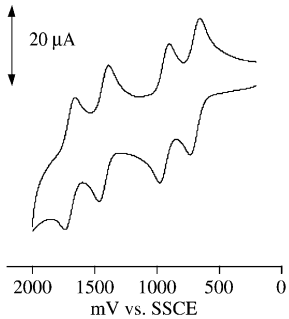

Figure 2. Cyclic voltammogram of $[Ru^{II}_2Fe^{II}_4(\mu\text{-}CN)_4(bpy)_8](PF_6)_4 \cdot CHCl_3 \cdot H_2O$ in CH_3CN containing 0.1M $[(tBu)_4N](PF_6)$ with a scan rate of 100 mV s^{-1} at 20 °C.

The CV of $[Ru^{II}Fe^{II}](PF_6)_4$ showed four quasireversible waves at 0.69, 0.94, 1.42 and 1.70 V (vs. SSCE). As shown by controlled potential coulometry at 2.0 V, the four quasireversible waves correspond to four one-electron processes: $[Ru^{II}_2Fe^{II}_2]^{4+} \rightleftarrows [Ru^{II}_2Fe^{II}Fe^{III}]^{5+} \rightleftarrows [Ru^{II}_2Fe^{III}_2]^{6+} \rightleftarrows [Ru^{II}Ru^{III}Fe^{III}_2]^{7+} \rightleftarrows [Ru^{III}_2Fe^{III}_2]^{8+}$. In the case of $[Fe^{II}_4](PF_6)_4$, the only

Table 2. Cyclic voltammetry data for $[Ru_2Fe_2(\mu\text{-}CN)_4(bpy)_8](PF_6)_4\cdot CHCl_3\cdot H_2O$ and related compounds.

Compound	$E_{1/2}$[a]		K_c
$[Ru^{II}(CN)_2(bpy)_2]$	0.83	Ru^{II}/Ru^{III}	
$[Fe^{II}(CN)_2(bpy)_2]$	0.47	Fe^{II}/Fe^{III}	
$[Ru^{II}_2Fe^{II}_4(\mu\text{-}CN)_4(bpy)_8](PF_6)_4$	0.69	$Ru^{II}_2Fe^{II}_2/Ru^{II}_2Fe^{II}Fe^{III}$	1.7×10^4
	0.84	$Ru^{II}_2Fe^{II}Fe^{III}/Ru^{II}_2Fe^{III}_2$	
	1.42	$Ru^{II}_2Fe^{III}_2/Ru^{II}Ru^{III}Fe^{III}_2$	
	1.70	$Ru^{II}Ru^{III}Fe^{III}_2/Ru^{III}_2Fe^{III}_2$	5.4×10^4
$[Fe^{II}_4(\mu\text{-}CN)_4(bpy)_8](PF_6)_4$	0.67	$Fe^{II}_4/Fe^{II}_3Fe^{III}$	2.4×10^3
	0.86	$Fe^{II}_3Fe^{II}/Fe^{II}_2Fe^{III}_2$	

[a] Volts vs. SSCE, a glassy carbon working electrode, CH_3CN containing 0.1M. $[n-Bu_4N]PF_6$, scan rate of 100 mV s^{-1}, 20 °C.

two quasireversible CV waves are observed at 0.67 and 0.86 V and correspond to two one-electron process: $[Fe^{II}_4]^{4+} \rightleftarrows [Fe^{II}_3Fe^{III}]^{5+} \rightleftarrows [Fe^{II}_2Fe^{III}_2]^{6+}$.[8] In $[Fe^{II}_4]^{4+}$, two of the coordination sites of the Fe^{2+} ions are occupied by either a cyanide carbon or nitrogen atom. The d orbitals of the Fe^{2+} ion coordinated with the cyanide carbon atoms are stabilised by π back donation, whereas the σ-donating character of the cyanide nitrogen destabilises the d orbitals of the Fe^{2+} ion.

Since the oxidations occur at a lower potential, the first two quasireversible waves were assigned to the Fe centres coordinated by cyanide N atoms. $[Ru^{II}Fe^{II}](PF_6)_4$ has two oxidation waves at similar potentials (0.69 and 0.84 V), therefore, these were assigned to the iron centres coordinated by the cyanide nitrogen atoms. This also supports the atom assignments in the X-ray analysis. Since the oxidation potential of the Ru monomer $[Ru^{II}(CN)_2(bpy)_2]$ (0.83 V) is higher than that of the Fe monomer $[Fe^{II}(CN)_2(bpy)_2]$ (0.47 V), the two waves at higher potential were assigned to the Ru^{II} centres. The trinuclear cyanide-bridged Ru^{II} complex [NC-Ru(bpy)$_2$-CN-Ru(bpy)$_2$-NC-Ru(bpy)$_2$-CN]$(PF_6)_2$ shows similar behaviour as well, and its CV waves at 0.66 and 1.19 V were assigned to the Ru^{II} ions coordinated with cyanide nitrogen and carbon atoms, respectively.[9]

The separation between the waves is a measure of the stability, imparted by electron delocalisation, of the mixed-valence species $[Ru^{II}_2Fe^{II}Fe^{III}]^{5+}$ and $[Ru^{II}Ru^{III}Fe^{III}_2]^{7+}$. This is generally represented as comproportionation constants (K_c) defined by the following Equations (1) and (2).

$$[Ru^{II}_2Fe^{II}_2]^{4+} + [Ru^{II}_2Fe^{III}_2]^{6+} \overset{K_c}{\rightleftharpoons} 2[Ru^{II}_2Fe^{II}Fe^{III}]^{5+} \quad (1)$$

$$[Ru^{II}_2Fe^{III}_2]^{6+} + [Ru^{III}_2Fe^{III}_2]^{8+} \overset{K_c}{\rightleftharpoons} 2[Ru^{II}Ru^{III}Fe^{III}_2]^{7+} \quad (2)$$

The observed peak separations of $\Delta E = 0.25$ and 0.28 V yield K_c values of 1.7×10^4 and 5.4×10^4 for Equations (1) and (2), respectively; this indicates an intermediate thermodynamic stability for the mixed valence species. On the other hand, the separation between the potentials for the second and the third oxidation steps is very large ($\Delta E = 0.48$ V) because the first two redox processes occur at the Fe sites and the last two at the Ru sites.

Controlled potential absorption spectra of $[Ru^{II}_2Fe^{II}_2](PF_6)_4$ in acetonitrile at −30 °C are shown in Figure 3. Table 3 summarises the UV data of $[Ru^{II}_2Fe^{II}_2](PF_6)_4$ together with that of $[Fe^{II}_4](PF_6)_4$.

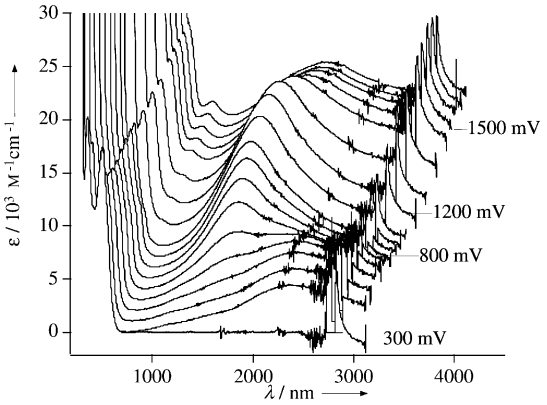

Figure 3. Electronic absorption spectra of $[Ru^{II}_2Fe^{II}_4(\mu\text{-}CN)_4(bpy)_8](PF_6)_4\cdot CHCl_3\cdot H_2O$ before and after electrolyses. Spectroelectrochemical experiments were carried out at −30 °C in an optically transparent thin-layer electrode made by placing a platinum grid between the windows of a 2 mm spectrophotometric cell directly mounted on a spectrophotometer. Electrochemical oxidations were carried out with the counter electrode, Pt wire, separated from the cathodic compartment by a frit and SSCE was used as a reference electrode.

The UV region is dominated by π–π* transitions of the bpy ligands, and the visible region consists of metal-to-ligand charge-transfer (d–π*) transitions. On electrochemical one-electron oxidation at 0.80 V (vs. SSCE) for $[Ru^{II}_2Fe^{II}_2](PF_6)_4$, the MLCT band ($\lambda_{max} = 500$ nm with $\varepsilon = 17400$ M^{-1} cm^{-1}) shifted to the blue with a decrease in its maximum ($\lambda_{max} =$ 470 nm with $\varepsilon = 13100$ M^{-1} cm^{-1}) as $[Ru^{II}_2Fe^{II}Fe^{III}]^{5+}$ was formed, and a new band grew in the near-IR region ($\lambda_{max} =$ 2350 nm with $\varepsilon = 5500$ M^{-1} cm^{-1}) after complete one-electron oxidation at 0.8 V. Further oxidation at 1.2 V causes the MLCT band to shift to the higher energy region with a decrease in intensity ($\lambda_{max} = 410$ nm with $\varepsilon = 10900$ M^{-1} cm^{-1}) and the formation of a new band at 1380 nm ($\varepsilon =$ 8600 M^{-1} cm^{-1}). In the CV, the first two redox waves (0.69 and 0.84 V) were assigned to one-electron processes occurring at the Fe centres ($Fe^{II/III}$), while the last two waves (1.42 and 1.70 V) were assigned to the redox processes at the Ru sites ($Ru^{II/III}$). The dπ orbitals of the ruthenium ions are considered to be more stabilised than those of the iron ions. The new

Table 3. Uv-visible data and mixed-valence parameters for $[Ru_2Fe_2(\mu\text{-}CN)_4(bpy)_8](PF_6)_4\cdot CHCl_3\cdot H_2O$ and related compounds.

Compound		ν_{max} [cm^{-1}]	ε [M^{-1}cm^{-1}]	$\Delta\nu_{1/2}$ [cm^{-1}]	H_{AB}	α^2
$[Ru^{II}_2Fe^{II}_2(\mu\text{-}CN)_4(bpy)_8](PF_6)_4$	$[Ru^{II}_2Fe^{II}Fe^{III}]^{5+}$	4260	5500	3000	1090	0.065
	$[Ru^{II}_2Fe^{III}_2]^{6+}$	6410	10500	3500	1990	0.096
$[Fe^{II}_4(\mu\text{-}CN)_4(bpy)_8](PF_6)_4$	$[Fe^{II}_2Fe^{III}_2]^{6+}$	7230	8600	1450	1230	0.028
$[(CN)_5Fe^{III}(\mu\text{-}NC)Fe^{II}(CN)_5]^{6-}$						0.03
$[(NC)Ru(bpy)_2(\mu\text{-}CN)Ru(bpy)_2CN]^{2+}$					2000	0.07

absorption bands (2350 and 1380 nm) appearing in the near-IR region after the electrolyses can, therefore, be attributed to intervalence transitions (IT) from the Fe^{II} to the Fe^{III} sites for the $[Ru^{II}_2Fe^{II}Fe^{III}]^{5+}$ state and from the Ru^{II} to the Fe^{III} sites for the $[Ru^{II}_2Fe^{III}_2]^{6+}$ state, respectively.

The values of the molar absorptivities and half-widths are related to the oscillator strength of the electronic transition. Applying the Hush equations[10] for mixed valence complexes, the electronic interaction matrix elements ($H_{AB} = 2.05 \times 10^{-2}\sqrt{\varepsilon_{max}\Delta\tilde{\nu}_{1/2}\tilde{\nu}_{max}}/r$) and the degrees of electronic delocalisation ($\alpha = (H_{AB}/\tilde{\nu}_{max})^2$) were estimated to be 1090 cm^{-1} and 0.065 for the $[Ru^{II}_2Fe^{II}Fe^{III}_2]^{5+}$ state and 1990 cm^{-1} and 0.096 for the $[Ru^{II}_2Fe^{III}_2]^{6+}$ states, respectively. In the calculation an intermetal separation of 5 Å obtained from the X-ray data was used, and the calculated parameters are listed in Table 3. The values of α^2 for the $[Ru^{II}_2Fe^{II}Fe^{III}]^{5+}$ and $[Ru^{II}_2Fe^{III}_2]^{6+}$ states are larger than the reported data for $[Fe^{II}_2Fe^{III}_2]^{6+}$ ($\alpha^2 = 0.03$) and the dinuclear complex $[(CN)_5Fe^{III}(NC)Fe^{II}(CN)_5]^{6-}$ ($\alpha^2 = 0.03$).[11] A small degree of delocalisation, which is comparable to the delocalisation in the dinuclear complex [NC-Ru(bpy)$_2$-(CN)-Ru(bpy)$_2$-CN]$^{2+}$($H_{AB} = 2000$ cm^{-1} and $\alpha^2 = 0.07$),[12] indicates class II behaviour.[13]

IR spectra: The CN-stretching frequencies of cyanide groups are generally sensitive to the bond lengths (d_{CN}) of the CN groups and to the oxidation state of the metal ions to which they are coordinated as well as the degree of M−CN back bonding across the ligand bridge.[14] The d_{CN} in $[Fe^{II}(CN)_2(phen)_2]$[15] and $[Fe^{III}(CN)_2(bpy)_2](ClO_4)$[16] are 1.149(7)–1.151(7) Å and 1.123(9)–1.135(1) Å, respectively. The former has strong ν(CN) signals at 2075 and 2062 cm^{-1}, while the latter has a very weak IR band at 2120 cm^{-1}.[9] Multiple absorption bands at 2083, 2112 and 2129 cm^{-1} were observed for $[Fe^{II}_4](PF_6)_4$. $[Ru^{II}_2Fe^{II}_2](PF_6)_4$ has a relatively strong IR peak at 2116 cm^{-1}, while the compound $[Ru^{II}(CN)_2(bpy)_2]$ has a strong band at 2060 cm^{-1}. The energy of the ν(CN) vibration frequency does not vary over a wide range for $[Fe^{II}_4](PF_6)_4$ and $[Ru^{II}_2Fe^{II}_2](PF_6)_4$, considering the different degrees of π-back bonding. The observed ν(CN) stretching frequencies for the squares are higher than those for the mononuclear complexes; this implies that there is weaker π-back donation in the squares. The CV data for $[Fe^{II}_4](PF_6)_4$ and $[Ru^{II}_2Fe^{II}_2](PF_6)_4$ suggest a large degree of π-back bonding and are inconsistent with the conclusion from the ν(CN) data. The energy of ν(CN) stretch in the squares depends on not only π-back donation but also on symmetry and kinematic coupling of the bridging cyanide caused by its constraint between two heavy metal ions.

Conclusion

Mixed-valence states in homometal systems are expected to have stronger IVCT interactions than heterometal systems. The IVCT interaction between cyanide-bridged ruthenium and iron ions is, however, found to be stronger than that between iron ions, due to the asymmetric bridging ligand CN^-. Cyanide ions have the potential to assemble metal ions and propagate not only magnetic but also electronic interactions, which are closely related. Combinations of a variety of metal ions can be introduced into the molecular squares, physical and chemical studies of which prompt the further understanding of metal-to-metal interactions mediated by cyanide bridges.

Experimental Section

Synthesis of $[Ru^{II}_2Fe^{II}_2(\mu\text{-}CN)_4(bpy)_8](PF_6)_4\cdot CHCl_3\cdot H_2O$: All chemicals were used as received without further purification, and all procedures were carried out under a nitrogen atmosphere. $AgNO_3$ (68 mg, 0.4 mmol) in ethanol (20 mL) was added to an ethanolic solution (20 mL) of $[RuCl_2(bpy)_2]_2\cdot H_2O$ (104 mg, 0.2 mmol). After the mixture had been stirred for three hours, AgCl was removed by filtration. $[Fe(CN)_2(bpy)_2]$ (85 mg, 0.2 mmol) was added to the resulting dark red solution, and the mixture was then heated under reflux for three days. NH_4PF_6 (130 mg, 0.8 mmol) was added to the dark red solution, and dark violet microcrystals were filtered by suction. Dark violet plates, suitable for X-ray analysis, were obtained by diffusion of acetonitrile solution with chloroform. Elemental analysis calcd (%) for $C_{84}H_{64}F_{24}Fe_2N_{20}P_4Ru_2$: C 44.89, H 2.87, N 12.47; found: C 44.75, H 2.84, N 12.31.

Electrochemical measurements and UV-visible spectra: Cyclic voltammetry (CV) and differential-pulse voltammetry (DPV) were carried out in nitrogen-purged acetonitrile solution at room temperature with use of a BAS CV-50W voltammetric analyser. A glassy carbon electrode was used as the working electrode. The counter electrode was a platinum coil, and the reference electrode was a saturated sodium calomel electrode (SSCE). The concentration of the complexes was 1×10^{-3} M, and tetrabutyl ammonium hexafluorophosphate (0.1M) was used as the supporting electrolyte. CV was performed at a scan rate of 100 $mV\,s^{-1}$. All the half-wave potentials $E_{1/2} = (E_{pc} + E_{pa})/2$, in which E_{pc} and E_{pa} are the cathodic and anodic peak potential, respectively, are reported with respect to the SSCE in this study. Controlled-potential absorption spectra were obtained with an optically transparent thin-layer electrode (OTTLE) cell. The working electrode was platinum mesh, and the counter electrode was a platinum coil. The reference electrode was an SSCE. Spectroelectrochemical measurements were carried out by using a Hokutodenko HA-501 potentiostat. The OTTLE cell was cooled to about −30 °C. All electrochemical and spectroelectrochemical measurements were carried out under a nitrogen atmosphere.

Crystallography: Crystallographic data are listed in Table 4. A single crystal ($0.04 \times 0.2 \times 02$ mm^3) was mounted with epoxy resin on the top of a glass fibre. The data were collected at −70 °C ($Mo_{K\alpha} = 0.71073$ Å) on a

Table 4. Crystal data and structure refinement for $[Ru_2Fe_2(\mu\text{-}CN)_4(bpy)_8](PF_6)_4\cdot CHCl_3\cdot H_2O$.

F_w	2453.07
T [°C]	−70
crystal system	triclinic
space group	$P\bar{1}$ (No.2)
a [Å]	13.505(2)
b [Å]	15.520(2)
c [Å]	24.405(4)
λ [°]	74.053(4)
λ [°]	79.401(4)
λ [°]	78.019(4)
V [Å^3]	4767.4(13)
Z	2
λ [Å]	0.71073
ρ_{calcd} [g cm^{-3}]	1.709
$\mu(Mo_{K\alpha})$ [mm^{-1}]	0.897
Transmission coeff.	0.880–1.000
$R1$[a]	0.088
$R2$[b]	0.241

[a] $R1 = \Sigma\,||F_o| - |F_c||/\Sigma|F_o|$. [b] $wR2 = [\Sigma[w(F_o^2 - F_c^2)^2]/\Sigma[w(F_o^2)^2]]^{0.5}$ and calcd $w = 1/[\sigma^2(F_o^2) + (0.1961\,P)^2]$.

Bruker SMART 1000 diffractometer fitted with a CCD-type area detector for by $\omega - 2\theta$ scan method, within the limits $2^\circ < \theta < 26^\circ$. A total of 23327 reflections were collected; this yielded 13318 ($R_{int} = 0.0461$) independent reflections. An empirical absorption correction was applied (SADABS). The structures were solved by direct methods and refined by the full-matrix least-squares method on all F^2 data with the SHELXTL 5.1 package (Bruker Analytical X-ray Systems). All non-hydrogen atoms were refined with anisotropic thermal parameters. Hydrogen atoms were included in calculated positions and refined with isotropic thermal parameters riding on those of the parent atoms. The relatively high R values are due to the low quality of the crystal and disorder of PF_6^- ions and solvent molecules.

CCDC-203551 contains the supplementary crystallographic data for this paper. These data can be obtained free of charge via www.ccdc.cam.ac.uk/conts/retrieving.html (or from the Cambridge Crystallographic Data Centre, 12 Union Road, Cambridge CB2 1EZ, UK; fax: (+44) 1223-336033; or deposit@ccdc.cam.uk).

Acknowledgements

This work was partially supported by the COE project at the University of Tsukuba and by a Grant-in-Aid for Scientific Research from the Ministry of Education, Science, Sports and Culture, Japan.

[1] a) D. W. Thompson, J. R. Schoonover, T. J. Meyer, R. A. Argazzik, C. A. Bignozzi, *J. Chem. Soc. Dalton Trans.* **1999**, 3729; b) C. A. Bignozzi, S. Roffia, C. Chiorboli, J. Davila, M. T. Indelli, F. Scandola, *Inorg. Chem*. **1989**, *28*, 4350; c) C. A. Bignozzi, S. Roffia, F. Scandola, *J. Am. Chem. Soc*. **1985**, *107*, 1644; d) B. W. Pfennig, V. A. Fritchman, K. A. Hayman, *Inorg. Chem*. **2001**, *40*, 244; e) S. Roffia, R. Casadei, F. Paolucci, C. Paradisi, *J. Electroanal. Chem*. **1991**, *302*, 157; f) A. Ferretti, A. Lami, M. J. Ondrechen, G. J. Villani, *J. Phys. Chem*. **1995**, *99*, 10484, and references therein; g) G. Rogez, A. Marvilliers, P. Sarr, S. Parsons, S. J. Teat, L. Ricard, T. Mallah. *Chem. Commun.* **2002**, 1460.

[2] a) A. Ito, M. Suenaga, K. Ono, *J. Chem. Phys.* **1968**, *48*, 3597; b) T. Mallah, S. Thiebaut, M. Verdaguer, P. Veillet, *Science* **1993**, *262*, 1554; c) W. R. Entley, G. S. Girolami, *Science* **1995**, *268*, 397; d) V. Gadet, T. Mallah, I. Castro, P. Veillet, M. Verdaguer, *J. Am. Chem. Soc*. **1992**, *114*, 9213; e) W. D. Griebler, D. Babel, *Z. Naturforsch*. **1982**, *87b*, 832; f) S. Ferlay, T. Mallah, R. Ouahès, P. Veillet, M. Verdaguer, *Inorg. Chem*. **1999**, *38*, 229; g) S. Ferlay, T. Mallah, R. Ouahès, P. Veillet, M. Verdaguer, *Science* **1995**, *378*, 701; h) O. Sato, T. Iyoda, A. Fujishima, K. Hashimoto, *Nature* **1996**, *271*, 49; i) W. R. Entley, G. S. Girolami, *Inorg. Chem*. **1994**, *33*, 5165; j) J. Larionova, R. Clérac, J. Sanchiz, O. Kahn, S. Golhen, L. Ouahab, *J. Am. Chem. Soc*. **1998**, *120*, 13088; k) A. N. Holden, B. T. Matthias, P. W. Anderson, H. W. Lewis, *Phys. Rev.* **1956**, *102*, 1463; l) R. M. Bozorth, H. J. Williams, D. E. Walsh, *Phys. Rev*. **1956**, *103*, 572.

[3] a) O. Sato, T. Iyoda, A. Fujishima, K. Hashimoto, *Science* **1996**, *272*, 704; b) M. Verdaguer, *Science* **1996**, *272*, 698.

[4] a) D. G. Fu, J. Chen, X. S. Tan, L. J. Jiand, S. W. Zhang, P. J. Zheng, W. X. Tang, *Inorg. Chem*. **1997**, *36*, 220; d) K. V. Langenberg, S. R. Batten, K. J. Berry, D. C. R. Hockless, B. Moubaraki, K. S. Murray, *Inorg. Chem*. **1997**, *36*, 5005.

[5] a) A. Scuiller, T. Mallah, M. Verdaguer, A. Nivorozkhin, J.-L. Tholence, P. Veillet, *New J. Chem*. **1996**, *20*, 1; b) T. Mallah, C. Auberger, M. Verdaguer, P. Veillet, *J. Chem. Soc. Chem. Commun*. **1995**, *1*, 61; c) N. Vernier, G. Bellessa, T. Mallah, M. Verdaguer, *Phys. Rev. B* **1997**, *56*, 75; d) J. L. Heinrich, J. J. Sokol, A. G. Hee, J. R. Long, *J. Solid State Chem.* **2001**, *159*, 293.

[6] a) G. Zhong, Z. J. Seino, Y. Mizobe, M. Hidai, A. Fujishima, S. Ohkoshi, K. Hashimoto, *J. Am. Chem. Soc*. **2000**, *122*, 2952; b) J. Larionova, M. Gross, M. Pilkington, H. Andres, H. Stoeckli-Evans, H. U. Güdel, S. Descurtins, *Angew. Chem*. **2000**, *112*, 1667; *Angew. Chem. Int. Ed*. **2000**, 39, 1605.

[7] a) J. J. Sokol, M. P. Shores, J. R. Long, *Inorg. Chem*. **2002**, *41*, 3052; b) P. A. Berseth, J. J. Sokol, M. P. Henrich, J. R. Long, *J. Am. Chem. Soc*. **2000**, *122*, 9655; c) J. J. Sokol, M. P. Shores, J. R. Long, *Angew. Chem*. **2000**, *113*, 242; *Angew. Chem. Int. Ed*. **2001**, *40*, 236.

[8] H. Oshio, H. Onodera, O. Tanmada, H. Mizutani, T. Hikichi, T. Ito, *Chem. Eur. J.* **2000**, *6*, 2523.

[9] a) V. Balzani, A Juris, M. Venturi, S. Campagna, S. Serroni, *Chem. Rev*. **1996**, *96*, 759; b) C. A. Bignozzi, J. R. Schoonover, F. Scandola, *Prog. Inorg. Chem*. **1997**, *44*, 1; c) C. A. Bignozzi, S. Roffia, C. Chiorboli, J. Davila, M. T. Indelli, F. Scandola, *Inorg. Chem*. **1989**, *28*, 4350.

[10] a) N. S. Hush, *Prog. Inorg. Chem*. **1967**, *8*, 391; b) C. Creutz, *Prog. Inorg. Chem*. **1983**, *30*, 1.

[11] R. Glauser, U. Hauser, F. Herren, A. Ludi, P. Roder, E. Schmidt, H. Siegenthaler, F. Wenk, *J. Am. Chem. Soc*. **1973**, *95*, 8458.

[12] C. A. Bignozzi, S. Roffia, C. Chiorboli, J. Davila, M. T. Indellim, F. Scandola, *Inorg. Chem*. **1989**, *28*, 4350.

[13] M. B. Robin, P. Day, *Adv. Inorg. Chem. Radiochem*. **1967**, *10*, 247.

[14] C. A. Bignozzi, R. Argazzi, J. R. Schoonover, K. C. Gordon, R. B. Dyer, R. B. Scandola, *Inorg. Chem.* **1992**, *31*, 5260.

[15] S. Zhan, Q. Meng, X. You, G. Wang, P. Zheng, *Polyhedron* **1996**, *15*, 2655.

[16] a) T.-H. Lu, H.-Y. Kao, D. I. Wu, K. C. Kong, C. H. Cheng, *Acta Crystallogr*. **1988**, *C44*, 1184, b) A. A. Schilt, *Inorg. Chem*. **1964**, *3*, 1323.

Received: February 20, 2003 [F4867]

